The Indonesian Journal of Computer Science
www.ijcs.net
Volume 15, Issue 1, February 2026
https://doi.org/10.33022/ijcs.v15i1.5056

Design of Brushless DC (BLDC) Motor Speed Control System Using Field Oriented Control (FOC) Method

Rokhmat Rizki Perkasa Putra[1], Rokhmat Febrianto[2*]
rperkasaputra@gmail.com[1], rokhmat.febrianto@prasetiyamulya.ac.id[2*]
[1]Department of Engineering Physics, Institut Teknologi Sepuluh Nopember, Indonesia
[2]Department of Computer Systems Engineering, Universitas Prasetiya Mulya, Indonesia

Article Information

Received : 2 Dec 2025
Revised : 10 Jan 2026
Accepted : 1 Feb 2026

Keywords

BLDC Motor, Field Oriented Control, Performance, Steady-state error.

Abstract

Research on environmentally friendly vehicles has highlighted Electric Vehicles (EVs), which utilize electric motors for propulsion. This study focuses on controlling a Brushless DC (BLDC) motor, a prevalent motor type in EVs, using the Field Oriented Control (FOC) method. The research aims to design and analyze the performance of this FOC-based speed control system. The system model and its control strategy were simulated in MATLAB/Simulink. Performance was evaluated under various speed setpoints (100, 200, and 300 rpm) and torque loads (2, 4, and 7 N.m). The results demonstrate that the proposed control system operates effectively, maintaining a steady-state error of less than 5% across all test conditions. Furthermore, all other performance parameters also remained below 5%, confirming the system's robustness and precision in regulating BLDC motor speed.

A. Introduction

Technological advancements continue to influence various aspects of modern life, leading to the emergence of increasingly sophisticated devices and systems. These advancements are the result of continuous development and refinement of earlier technologies. In the transportation sector, conventional vehicles powered by petroleum-based fuels are still widely used in Indonesia. However, the reliance on petroleum, an exhaustible and non-renewable resource, has intensified efforts to explore and promote alternative, renewable energy sources. From this, there is a lot of research related to environmentally friendly vehicles, one of which is Electric Vehicle (EV). [1]

EVs or electric vehicles are vehicles that use electricity as fuel or energy to move. Because it uses electricity, the driving device used in EVs is an electric motor [2]. As the name suggests, electric motors can move because there is an electric current that moves the rotor or the part of the motor that can rotate. This movement can occur due to the lorentz force. [3]. Various types of electric motors have been developed over time. But in general, electric motors are classified into two main categories, namely AC motors and DC motors [4].

From the DC motor category, there are BLDC motors or Brushless DC Motors. BLDC motor is a type of DC (Direct Current) motor that does not have brushes (Brushless) on the rotor for commutation. In BLDC motors, the brushes on the commutator are replaced with electronic commutators so that the rotor is not connected to the power supply. BLDC motors have many advantages over DC motors with brushes including longer life, better speed and torque characteristics, less noise, and better efficiency [5].

The development of BLDC motor control systems can be done with various methods. One method that has been applied in previous research is Field oriented control (FOC). The FOC method is a BLDC motor control method that controls the current on the direct (id) and quadrature (iq) axes to obtain the desired speed [6]. The use of the FOC method to control BLDC motors has many advantages, namely with the FOC method, the response of BLDC motors will be faster and more dynamic than control in general. In addition, by using the FOC method, the ripple in the torque reading results will be reduced when compared to the six-step commutation method [7]. Therefore, in this study, the design of BLDC motor speed control using Field Oriented Control (FOC) method is carried out.

B. Research Method

The study titled “Design of a BLDC Motor Speed Control System Using the Field Oriented Control (FOC) Method” was conducted following the workflow illustrated in Figure 1.

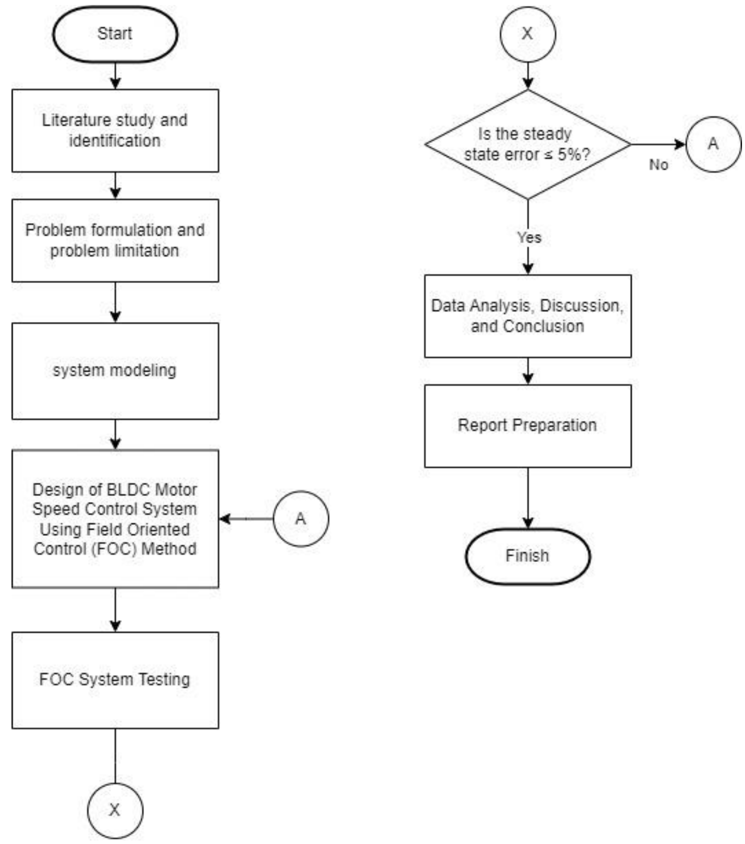

Figure 1. Research Flowchart

a. BLDC Motor Modeling

BLDC Motor Modeling is the process of creating a simulator representation of a system. In this study, the simulator in question is a BLDC motor plant. Meanwhile, in this study the system used is a BLDC motor speed control system using the Field Oriented Control or FOC method. The modeling made is a mathematical modeling of the FOC method for controlling BLDC motors. This modeling will be used in simulations performed on Simulink. The mathematical modeling of the BLDC motor can be described as follows.

$$\dot{x} = Ax + Bu \quad (1)$$

$$y = Cx + Du \quad (2)$$

Then from the initial mathematical equation of the BLDC motor, the following equation is obtained

$$\dot{i_a} = \frac{V_{as} - R_s i_a - e_a}{L - M} \quad (3)$$

$$\dot{i_b} = \frac{V_{bs} - R_s i_b - e_b}{L-M} \quad (4)$$

$$\dot{i_c} = \frac{V_{cs} - R_s i_c - e_c}{L-M} \quad (5)$$

Description:

V_{as}, V_{bs}, V_{cs}	= Stator voltage of each phase (V)
R_s	= Stator resistance per phase (Ohm)
i_a, i_b, i_c	= L = Stator phase current (A)
L_{aa}, L_{bb}, L_{cc}	= Self-inductance of each phase a, b, and c (H)
$L_{ab}, L_{ba}, L_{ac}, L_{ca}, L_{bc}, L_{cb}$	= M = Mutual inductance between phases a, b and c (H)
e_a, e_b, e_c	= Back-EMF force per phase (V)

So that the BLDC motor model equations can be described in Equations (6) and (7)

$$\begin{bmatrix} \dot{i_a} \\ \dot{i_a} \\ \dot{i_a} \\ \dot{\omega} \end{bmatrix} = \begin{bmatrix} A_{11} & 0 & 0 & 0 \\ 0 & A_{12} & 0 & 0 \\ 0 & 0 & A_{13} & 0 \\ 0 & 0 & 0 & \frac{d}{dt} \end{bmatrix} \begin{bmatrix} i_a \\ i_b \\ i_c \\ \omega \end{bmatrix} + \begin{bmatrix} B_{11} & 0 & 0 \\ 0 & B_{12} & 0 \\ 0 & 0 & B_{13} \\ 0 & 0 & 0 \end{bmatrix} \begin{bmatrix} V_{as} \\ V_{bs} \\ V_{cs} \end{bmatrix} \quad (6)$$

$$\begin{bmatrix} i_d \\ i_q \\ \omega \end{bmatrix} = \begin{bmatrix} \cos\theta & \cos\left(\theta - \frac{2\pi}{3}\right) & \cos\left(\theta + \frac{2\pi}{3}\right) & 0 \\ \sin\theta & \sin\left(\theta - \frac{2\pi}{3}\right) & \sin\left(\theta + \frac{2\pi}{3}\right) & 0 \\ 0 & 0 & 0 & 1 \end{bmatrix} \begin{bmatrix} i_a \\ i_b \\ i_c \\ \omega \end{bmatrix} \quad (7)$$

Where id is the current in the d (direct) axis and iq is the current in the q (quadrature) axis and,

$$A_{11} = \left(1 \times \frac{-R_s}{L-M}\right) - \frac{e_a}{L-M}$$

$$A_{12} = \left(1 \times \frac{-R_s}{L-M}\right) - \frac{e_b}{L-M}$$

$$A_{13} = \left(1 \times \frac{-R_s}{L-M}\right) - \frac{e_c}{L-M}$$

$$B_{11} = \frac{1}{L-M}$$

$$B_{12} = \frac{1}{L-M}$$

$$B_{13} = \frac{1}{L-M}$$

The BLDC motor utilized in this study operates based on the specifications listed in Table 1.

Table 1. BLDC motor specifications

Drive Motor	Dual BLDC Hub Motor
Motor Output Power	1,5 kW (3kW total)
Transmission	On Wheel
Gear Ratio	1 : 1
Driving Mode	Eco
Battery	Li-Ion 60V 30Ah
Maximum Speed	600 RPM
Acceleration (0-60 Km/h)	15 seconds
Maximum Torque	20 N.m
Rated Torque	7 N.m
Rated Current (A)	40
Dimensions (L × W × H, cm)	148, 60, 100
Wheel Base (cm)	120
Weight (kg)	70
Maximum Load Capacity (kg)	80
Phase Resistance (UV, VW, UW), (Ω)	1,86; 1,87; 1,89
Phase Inductance (UV, VW, UW), (μH)	241; 245,2; 238,9
Pole pairs	24

b. System design

System design is done by modeling and simulating in Simulink-Matlab software. The design begins with making a scheme or block diagram of FOC. The block diagram made for BLDC motor speed control with the FOC method can be seen in Figure 2.

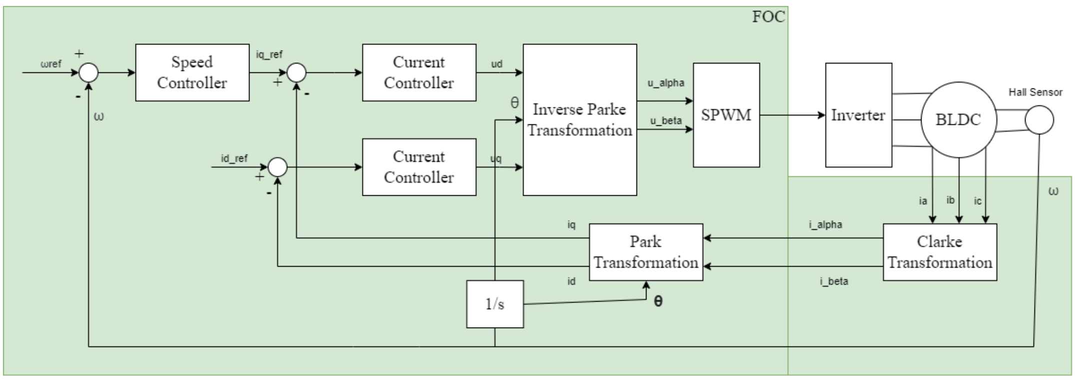

Figure 2. Block diagram of the proposed system

In Figure 2 the green shaded part is the block diagram of the FOC method, while the non-shaded part is the block diagram of the plant. The block diagram part that includes how the FOC method is carried out, has blocks including the controller block where the controller used is a PI controller, then the park transformation block, the clark transformation block, and the inverse parke transformation block.

While the block diagram section that includes the plant of the system, there are bldc motors, inverters, and hall sensors. The hall sensor here is used to directly measure the angular velocity of the motor, and the sensor is assumed to have a 1 to 1 ratio between the actual angular velocity and the measured angular velocity.

c. FOC system testing

Testing of the controller that uses the FOC method in its manufacture will be tested. Testing the FOC system is carried out with the aim of validating the speed readings. In this test, the feasibility of the system will also be tested by calculating the error on the speed set point that has been set with the speed output issued by the motor, if the calculation of the steady state error is below 5% then the system is considered feasible to apply. This FOC system test is divided into two tests, namely the speed variation test and the loading test. The speed variations used are 200 rpm, 400 rpm, and 600 rpm. Meanwhile, the load torque variations used are 2 N.m, 4 N.m, and 7 N.m.

C. Result and Discussion

a. BLDC Motor Simulation Results

Simulations are carried out with existing parameters, both existing (motor specifications) and those determined in advance. In addition, simulations are carried out in MATLAB 2023b software on one of its features, Simulink. The following are some of the results of the BLDC Motor simulation that has been carried out.

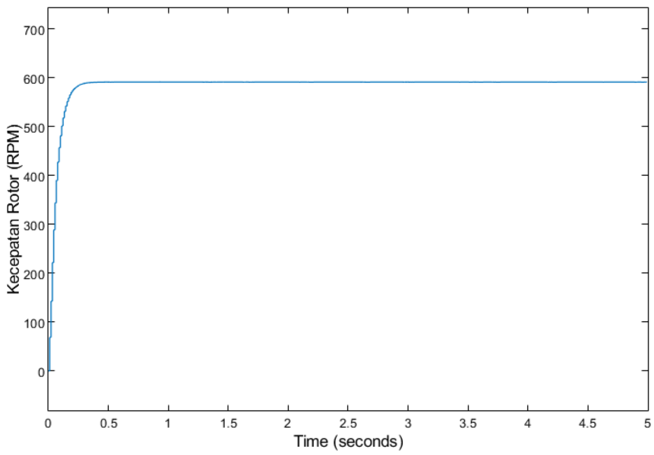

Figure 3. Speed respond of the Plant

Figure 3 is the result of the plant speed response that is run in open loop. From the graph it can be seen that the desired speed is 600 rpm. However, the speed achieved at steady state is 590.7 rpm after 0.4 seconds from the start of the run. From the results shown with the graph in Figure 3, it can be seen that the modeling error has a value of about 1.6%. This value is obtained by comparing the speed achieved in Figure 3 with the desired speed set point. With a modeling error value of less than 5%, the research can be continued with the design of a BLDC motor speed control system using the Field Oriented Control (FOC) method.

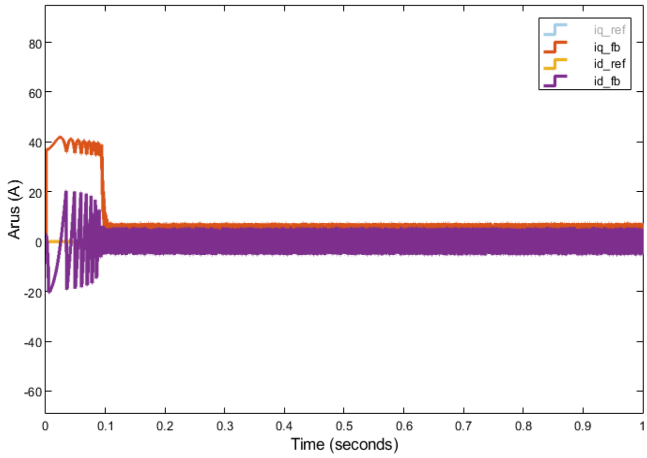

Figure 4. Dynamic current response of the control system

Figure 4 shows the dynamic response of the direct current and quadrature current. From the previous chapter, it is known that the quadrature current is the current that will be responsible for the motor torque while the direct current is responsible for the motor flux. So from this knowledge what you want to do is to make the direct current remain at zero value and then control the quadrature current to be at the maximum value. The maximum value here if described in the transverse view of the BLDC motor, the quadrature current is controlled so that the rotating magnetic field in the stator is 90 degrees ahead of the current rotor position, this causes the resulting torque to be at the maximum value. From the graph in Figure 4 it can be seen if the reference current of the direct current is still made zero while the quadrature current is not. it is because the quadrature current will produce electromagnetic torque and for the direct current is made zero because to maximize the torque generation of the quadrature current. The maximum or minimum torque produced also affects how far (degree) the quadrature current is separated from the direct current.

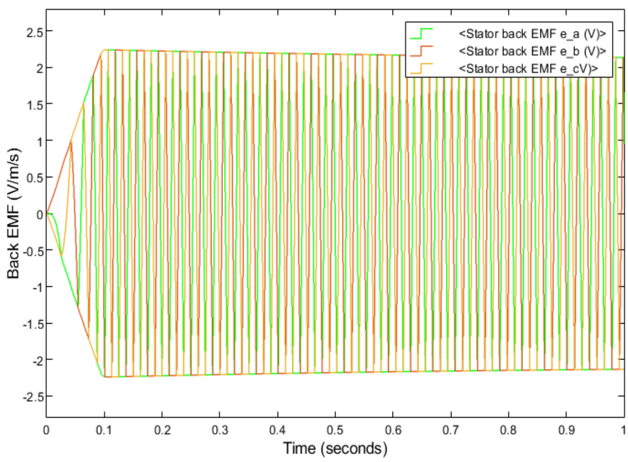

Figure 5. Dynamic BEMF response of the control system

Then in Figure 5 shows the dynamic response of BEMF or Back EMF (back emf) generated from the BLDC motor plant. From the graph in Figure 5, the back emf value starts from zero because at that time the motor still has zero speed and current. As the system continues to run, the current will continue to rise to generate a magnetic field in the stator. The value of the current to generate the magnetic field in the stator is adjusted to the speed value that you want to generate as well. The current will continue to be generated as in Figure 4 and will continue to stabilize at that value until the desired speed is reached. From Figures 4 and 5, it can be seen that the speed reached at 0.1 seconds is appropriate or exceeds the desired speed. From second 0.1 the current generated will be zero because there is no speed to be increased. Starting from second 0.1 Back emf is useful for maintaining the speed value at the desired value. If later when the speed is at a steady state or after the back emf continues to maintain the speed value according to the set point, there is an additional torque load on the motor. So to return the speed to the original value or in accordance with the set point, the current is generated again.

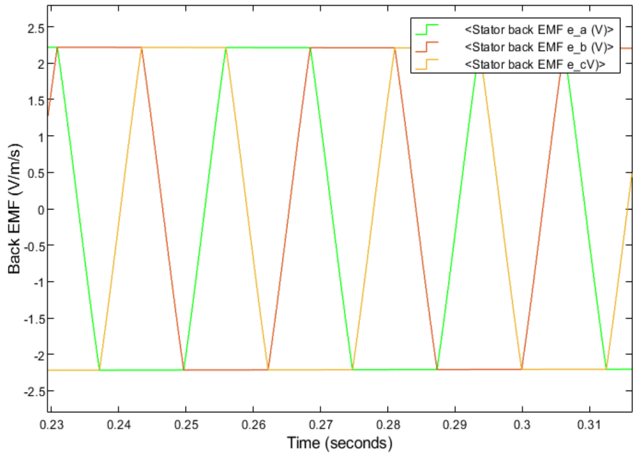

Figure 6. Shape of BEMF signal from BLDC motor

Then in Figure 6 shows the graph of the signal shape of the Back EMF generated from the BLDC motor. From the previous chapters, it can be seen that the Back EMF signal shape of the BLDC motor is trapezoidal. This signal shape is different from synchronous motors that are similar to BLDC motors, namely PMSM motors or Permanent Magnet Synchronous Motors. PMSM motors have a Sinusoidal Back EMF signal shape. The difference is caused by the conductor winding process on the stator, in BLDC motors, the type of winding used is concentrated windings or concentrated windings, while in PMSM motors, the type of winding used is distributed windings or distributed windings.

b. Control System Test Results with Speed Variation

The control system test with speed variations is carried out by simulating each predetermined speed input variation. This test was carried out with the aim of knowing the system response to each speed variation given. Simulation is done by giving speed variations of 200 rpm, 400 rpm, and 600 rpm to the system set points in simulink that have been designed before. The speed set points are connected to the speed controller as in the block diagram in Figure 3.2. Then the set points on the direct current are made zero as in chapter 3 and the input load torque or load torque is made zero. From this configuration, the system created in simulink is then run with a simulation time or stop time of 5 seconds.

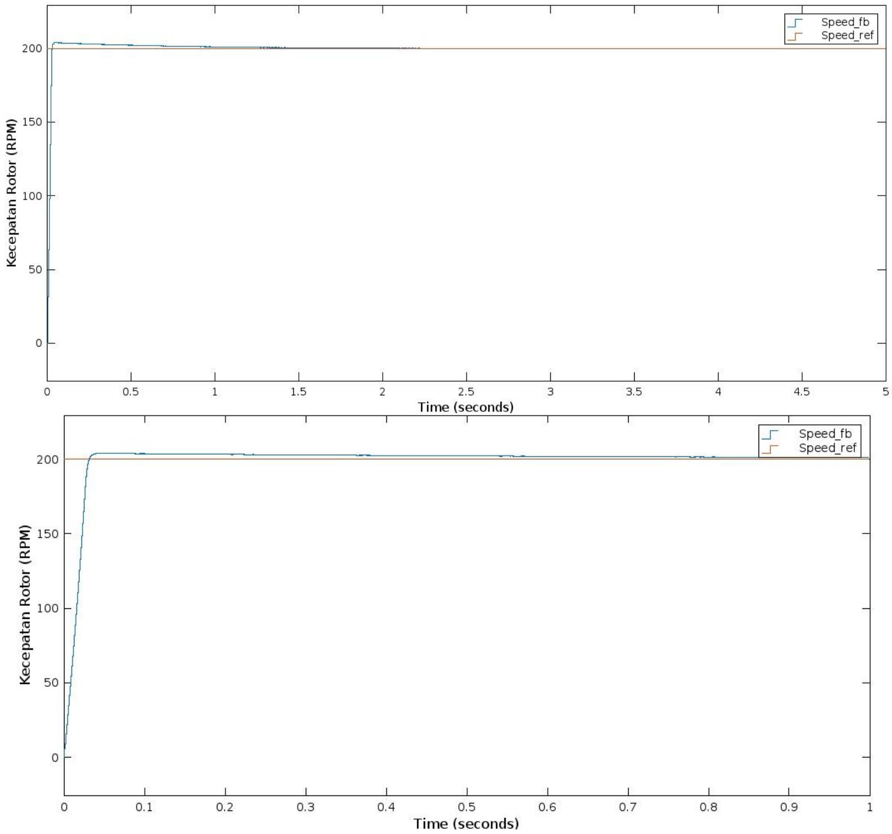

Figure 7. Dynamic speed response of the system with 200 rpm speed setpoint

Figure 7 shows the dynamic speed response of the designed system by giving a speed set point of 200 rpm. Figure 7 has 2 graphs where the top graph is the original graph according to the initial configuration of the control system test with speed variations characterized by a long simulation time of 5 seconds, while the bottom graph is a graph of the results of the magnification of the top graph where it can be seen if the rise time of the system with a set point speed of 200 rpm is 0.04 seconds and for the max overshoot value is at 0.04%.

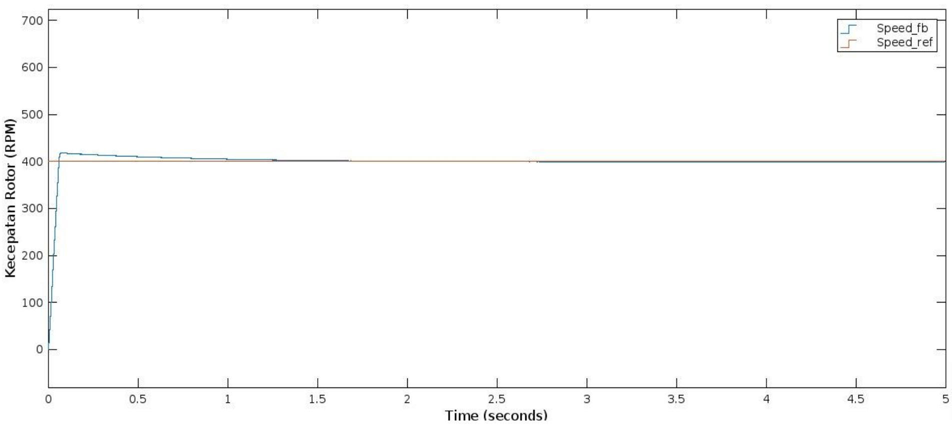

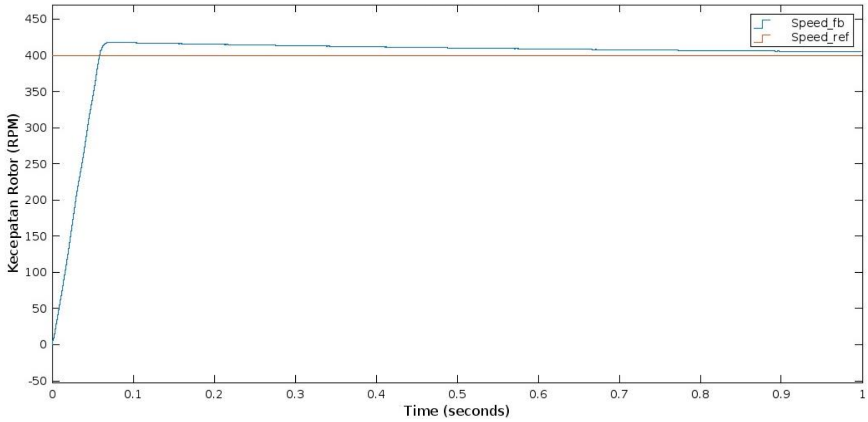

Figure 8. Dynamic speed response of the system with 400 rpm speed setpoint

Figure 8 shows the dynamic speed response of the designed system by giving a speed set point of 400 rpm. Figure 8 has 2 graphs where the top graph is the original graph according to the initial configuration of the control system test with speed variations characterized by the length of the simulation time is 5 seconds, while the bottom graph is a graph of the results of the magnification of the top graph where it can be seen if the rise time of the system with a speed set point of 400 rpm is 0.07 seconds and for the max overshoot value is at 0.08%.

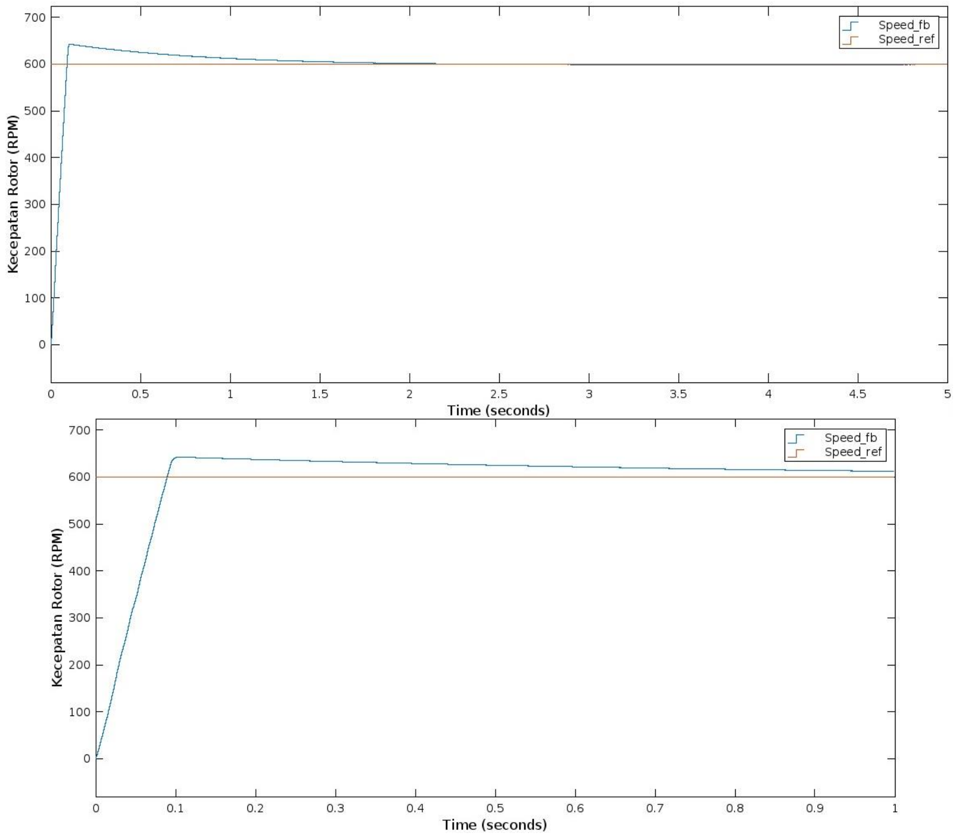

Figure 9. Dynamic speed response of the system with 600 rpm speed setpoint

Figure 9 shows the dynamic speed response of the designed system by giving a speed set point of 600 rpm. Figure 9 has 2 graphs where the top graph is the original graph according to the initial configuration of the control system test with speed variations characterized by the length of the simulation time is 5 seconds, while the bottom graph is a graph of the results of the magnification of the top graph where it can be seen if the rise time of the system with a speed set point of 600 rpm is 0.09 seconds and for the max overshoot value is at 0.083%.

The performance results and steady state errors for all speed variations are presented in Table 2 and Table 3, respectively.

Table 2. Performance of the designed Control System

RPM	Parameter	Result
	Rise Time	0,04 seconds
200	*Settling Time*	2,2 seconds
	Max. Overshoot	0,04%
	Rise Time	0,07 seconds
400	*Settling Time*	2,1 seconds
	Max. Overshoot	0,08%
	Rise Time	0,09 seconds
600	*Settling Time*	2,1 seconds
	Max. Overshoot	0,083%

Table 3. Error steady state (ess) of the designed control system

set point (rpm)	Simulation Result (rpm)	ess (%)
200	201,8	0,01
400	410,3	0,05
600	617,6	0,02

c. Control System Loading Test Results

The loading test is carried out by giving a torque load to the BLDC motor. Giving this torque load is done when the system is already in a steady or steady state, it is intended to determine the dynamic response of the control system when given a torque load with a load variation of 2 N.m, 4 N.m, 7 N.m. and with the same speed set point of 600 rpm.

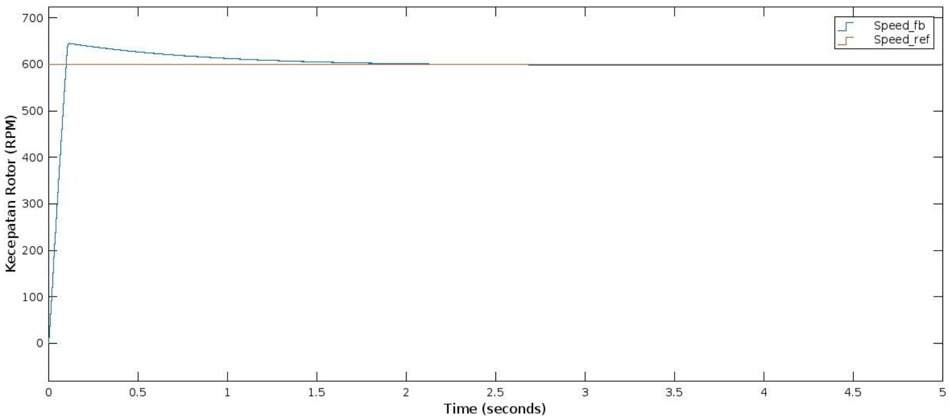

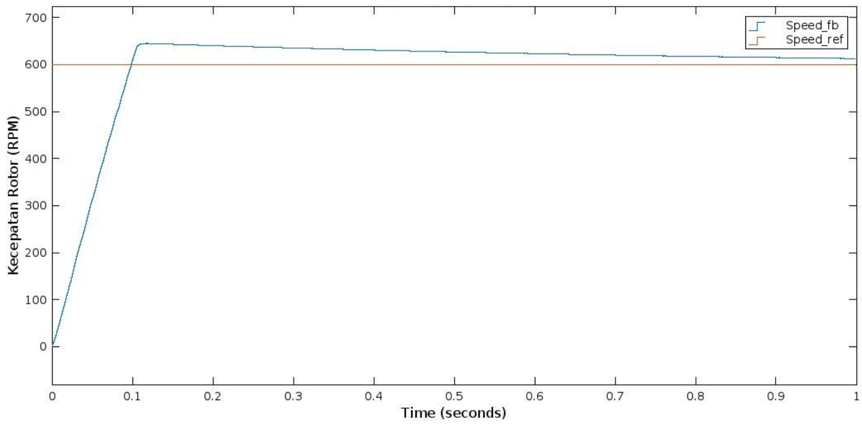

Figure 10. Dynamic speed response of the system with 2 N.m Load variation.

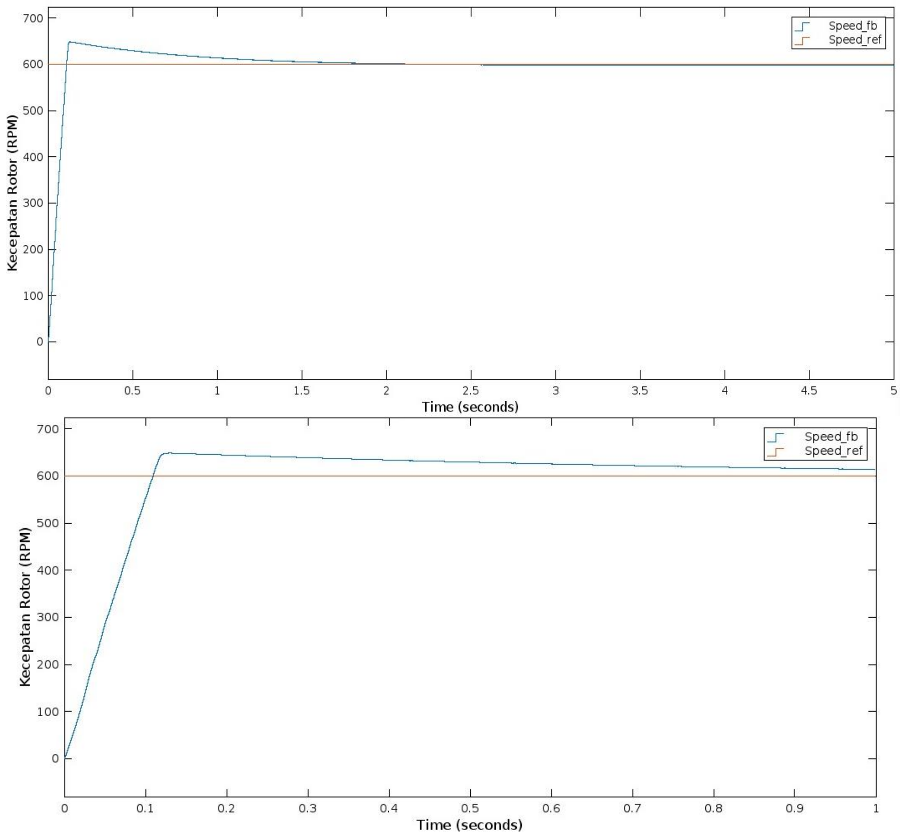

Figure 11. Dynamic speed response of the system with 4 N.m Load variation.

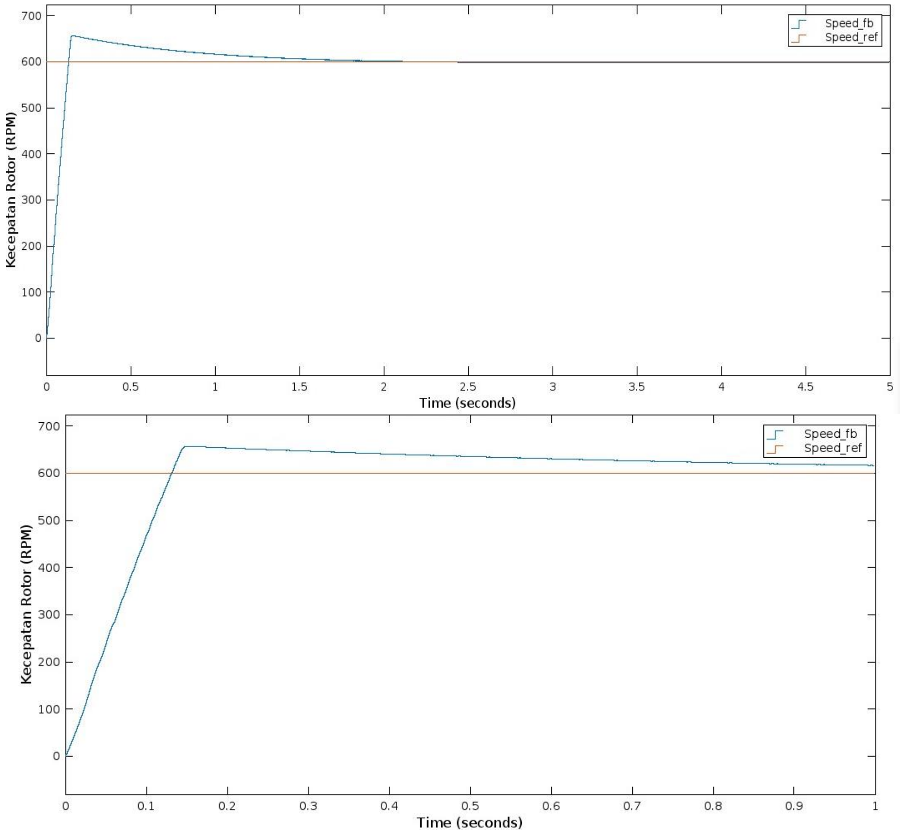

Figure 12. Dynamic speed response of the system with 7 N.m Load variation.

Figures 10, 11, and 12 show the graphical results of the control system loading test. The speed variations used in this test remain the same, namely 200 rpm, 400 rpm, and 600 rpm sequentially in Figures 10, 11, and 12. Some important points from the results of this test can be seen in the graph of the test results, namely the Max Overshoot value and the steady state error value. Max Overshoot value or overshoot percent is quite high and exceeds 5% in all variations. As for the steady state error value, this system has a fairly small error. The performance results and steady state errors on all speed variations are then presented in Table 4 and Table 5, respectively.

From the performance results presented in table 4. The system has good performance because it has quite low Rise Time, Settling Time, and Max Overshoot values in the range of 0.11 seconds; 2.1 seconds; and 0.08%, respectively. From these results, the addition of torque load on the motor does not seem to have a significant effect on the running or performance of this control system, this is reinforced by the graphs produced in Figures 10, 11, and 12 which have very similar graphs to each other.

Table 4. Performance of the designed control system when given a load

T_L	**Parameter**	**Result**
	Rise Time	0,04 seconds
2 N.m	*Settling Time*	2,2 seconds
	Max. Overshoot	0,04%
	Rise Time	0,07 seconds
4 N.m	*Settling Time*	2,1 seconds
	Max. Overshoot	0,08%
	Rise Time	0,09 seconds
7 N.m	*Settling Time*	2,1 seconds
	Max. Overshoot	0,083%

Table 5. *Error steady state* (ess) of the designed control system when given a load

T_L	**Result Simulasi (rpm)**	**ess (%)**
2 N.m	618,4	0,02
4 N.m	620,6	0,02
7 N.m	619,9	0,02

D. Conclusion

Based on the simulation results and the preceding analysis, the study successfully demonstrates the design and implementation of a BLDC motor speed control system using the Field Oriented Control (FOC) method. The proposed system integrates several key components, including a PI-based speed controller, an inverter for processing control signals, position sensors for obtaining rotor angle information, and the BLDC motor itself. The FOC strategy operates by transforming the three-phase motor currents into the d-q reference frame, enabling independent control of flux and torque-producing currents. The simulation outcomes indicate that the system achieves a notably small steady-state error of approximately 0.02%, confirming the accuracy and stability of the control approach.

Furthermore, the performance evaluation shows that the system exhibits favorable dynamic characteristics under both speed variation and load disturbance conditions. During the speed variation tests, the system demonstrates rapid rise times, short settling times, and minimal overshoot, with typical values of 0.07 seconds, 2.15 seconds, and 0.06%, respectively. Similarly, in the loading tests, the system maintains stable performance with rise times around 0.11 seconds, settling times of approximately 2.1 seconds, and overshoot values remaining below 0.1%. These results indicate that changes in speed demands and the application of additional torque loads do not significantly affect the dynamic behavior or overall performance of the control system. The findings affirm that the FOC-based control strategy provides robust and reliable speed regulation for BLDC motor applications.

E. Acknowledgment

The authors would like to acknowledge the support provided by the Department of Engineering Physics, Institut Teknologi Sepuluh Nopember, for facilitating the resources and academic environment required to conduct this research. Appreciation is also extended to all contributing units and individuals whose assistance, although not mentioned individually, has been valuable to the completion of this work.

F. References

[1] M. S.Patil and S.S.Dhamal, "A Detailed Motor Selection for Electric Vehicle Traction System," Third International conference on I-SMAC (IoT in Social, Mobile, Analytics and Cloud) (I-SMAC), pp. 679-684, 2019.

[2] G. Amar, G. Ismail and B. Riad, "Suitability of Electric Motors and Conventional Control Techniques for Electric Vehicle Applications," International Conference of Advanced Technology in Electronic and Electrical Engineering (ICATEEE), pp. 1-6, 2022.

[3] S. Ueno and T. Kato, "A novel design of a Lorentz-force-type small self-bearing motor," in International Conference on Power Electronics and Drive Systems (PEDS), Taipei, Taiwan, 2009.

[4] Z. Cao, A. Mahmoudi, S. Kahourzade and W. L. Soong, "An Overview of Electric Motors for Electric Vehicles," in Australasian Universities Power Engineering Conference, AUPEC, Perth, Australia, 2021.

[5] N. Prabhu, R. Thirumalaivasan and B. Ashok, "Critical Review on Torque Ripple Sources and Mitigation Control Strategies of BLDC Motors in Electric Vehicle Applications," IEEE Access, pp. 115699-115739, 2023.

[6] M. R. Fadli, M. M. Musyasy, J. Furqani and A. Purwadi, "Modelling of Field Orientation Control (FOC) Method in 120 kW Brushless DC Motor (BLDC)," in International Conference on Electric Vehicular Technology (ICEVT), Bali, Indonesia, 2019.

[7] R. Jauhar, N. Ismail and N. Sartika, "Design of Torque Controller Based on Field Oriented Control (FOC) Method on BLDC Motor," in International Conference on Telecommunication Systems, Services, and Applications (TSSA), Lombok, Indonesia, 2022.

[8] M. Lazor and M. Štulrajter, "Modified field oriented control for smooth torque operation of a BLDC motor," in ELEKTRO, Rajecke Teplice, Slovakia, 2014.

[9] H. Suryoatmojo, F. G. Cladella, V. Lystianingrum, D. Riawan, R. Mardiyanto and D. Ariana, "Performance of BLDC Motor Speed Control Based on Hysteresis Current Control Mechanism," in International Seminar on Intelligent Technology and Its Applications (ISITIA), Bali, Indonesia, 2018.

[10] A. Usman and B. S. Rajpurohit, "Effect of Stator Fault Currents on Rotor Permanent Magnets for a SPM-type BLDC Motor," in IEEE Industry Applications Society Annual Meeting (IAS), Detroit, MI, USA, 2020.

[11] D. A. Asfani, I. M. Y. Negara, I. G. N. S. Hernanda, D. Fahmi, M. C. Sihombing and P. M. T. Dewi, "BLDC Performance Analysis Due to Stator Winding Unbalance,"

in International Seminar on Intelligent Technology and Its Applications (ISITIA), Surabaya, Indonesia, 2021.

[12] T. Wang, Z. Ye, G. Sinha and X. Yuan, "Output Filter Design for a Grid-interconnected Three-phase Inverter," in Annual IEEE Conference on Power Electronics Specialists (PESC), Acapulco, Mexico, 2003.

[13] I. Mishra, M. Singh and D. Roy, "Comparative Evaluation of Different Pulse Width Modulation Techniques on VSI Fed Three Phase Induction Motor," in Recent Advances on Engineering, Technology and Computational Sciences (RAETCS), Allahabad, India, 2018.

[14] MathWorks, "Six Step Commutation," MathWorks, Natick, Massachusetts, USA, 2023.

[15] S.-C. Chen and D. S. Putra, "Machine Learning Implementation on BLDCM Commutation," in IEEE Eurasia Conference on Biomedical Engineering, Healthcare and Sustainability (ECBIOS), Tainan, Taiwan, 2020.

[16] M. Khalid, A. Mohan and B. A. C, "Performance Analysis of Vector controlled PMSM Drive modulated with Sinusoidal PWM and Space Vector PWM," in Power and Renewable Energy Conference (IPRECON), IEEE International, Karunagappally, India, 2020.

[17] S. Rajinth, C. Abeykoon and D. H. S. Maithripala, "Design of a Sensorless Field Oriented Control Drive for Brushless," in The 9th International Conference of Control, Dynamic Systems, and Robotics (CDSR'22), Niagara Falls, Canada, 2022.

[18] P. Yedamale, "Using the PIC18F2431 for Sensorless BLDC Motor Control," Microchip Technology, Dallas, Texas, U.S., 2005.

[19] Arduino.cc, “What Is Arduino? | Arduino Documentation,” docs.arduino.cc, Jan. 25, 2022. https://docs.arduino.cc/learn/starting-guide/whats-arduino/.